

## Proximity of Pseudogapped Superconductor and Commensurate Antiferromagnet in a Quasi-Two-Dimensional Organic System

K. Miyagawa,<sup>1</sup> A. Kawamoto,<sup>2</sup> and K. Kanoda<sup>1</sup>

<sup>1</sup>*Department of Applied Physics, University of Tokyo, Bunkyo-ku, Tokyo 113-8656, Japan*

<sup>2</sup>*Department of Physics, Hokkaido University, Sapporo 060-0810, Japan*

(Received 16 August 2001; published 14 June 2002)

We performed the single-crystal  $^{13}\text{C}$  NMR studies on a quasi-two-dimensional system, deuterated  $\kappa$ -(BEDT-TTF) $_2\text{Cu}[\text{N}(\text{CN})_2]\text{Br}$ , which is just on the border of the Mott transition. The NMR spectra are separated into two parts coming from the metallic (superconducting) and insulating phases due to the phase separation at low temperature. The examination of the separated spectra revealed that the Mott transition in this system is characterized by the first-order transition between the pseudogapped superconductor and the simplest commensurate antiferromagnet with a moment of  $0.26\mu_B/\text{dimer}$ .

DOI: 10.1103/PhysRevLett.89.017003

PACS numbers: 74.25.Nf, 71.30.+h, 74.70.Kn, 76.60.-k

The organic conductors exhibit a variety of ground states such as spin density wave (SDW), charge density wave, spin-Peierls, magnetically ordered, metallic, and superconducting states. The ground state is determined by the mutual interplay between the electron correlations, the electron-phonon interaction, the electron kinetic energy, and characteristics of the Fermi surfaces topology. In a family of the quasi-two-dimensional  $\kappa$ -(BEDT-TTF) $_2X$ , the role of the electron correlations is highlighted by the previous works [1–6], where BEDT-TTF is bis(ethylenedithio)tetrathiafulvalene as shown in Fig. 1(a). The  $\kappa$ -type molecular arrangement is characterized by strong dimerization of BEDT-TTF molecules in the two-dimensional layer [see Fig. 1(b)]. As a hole is introduced to a dimer from the monovalent anion,  $X^{-1}$ , an antibonding molecular orbital in the BEDT-TTF dimer is believed to be half filled. While the  $X = \text{Cu}[\text{N}(\text{CN})_2]\text{Br}$  and  $\text{Cu}(\text{NCS})_2$  salts are 10 K-class superconductors (SC), the  $X = \text{Cu}[\text{N}(\text{CN})_2]\text{Cl}$  salt is an antiferromagnetic insulator (AFI). The  $^{13}\text{C}$  and  $^1\text{H}$  NMR studies reveal that the antiferromagnetic spin fluctuations are enhanced commonly for all these members [3–5], among which only the insulating  $\text{Cu}[\text{N}(\text{CN})_2]\text{Cl}$  salt has a commensurate magnetic ordering at low temperatures [6]. Pressurizing this compound drives the insulating phase into the superconducting phase with a transition temperature  $T_C$  of  $\sim 13$  K (at  $\sim 1.3$  kbar) [7–10]. These facts indicate that the family of  $\kappa$ -(BEDT-TTF) $_2X$  are situated around the Mott transition and that the relative strength of the Coulomb interaction to the bandwidth is varied across a certain critical value by chemical substitution for  $X$  or physical pressure. Investigation of this family in the vicinity of the metal-insulator ( $M$ - $I$ ) transition is expected to make a significant contribution to the physics of the bandwidth-varied Mott transition with the band filling fixed at a half in two dimensions.

Previously, the deuterated  $\kappa$ -(BEDT-TTF) $_2$ - $\text{Cu}[\text{N}(\text{CN})_2]\text{Br}$  (which is denoted by  $d8$ - $\text{Cu}[\text{N}(\text{CN})_2]\text{Br}$  and the nondeuterated salt is by  $h8$ - $\text{Cu}[\text{N}(\text{CN})_2]\text{Br}$  hereafter) is found to be situated just on the  $M$ - $I$  boundary by

the  $^{13}\text{C}$  NMR,  $^1\text{H}$  NMR, and susceptibility measurements for the powdered sample [11]. In this Letter, the single-crystal  $^{13}\text{C}$  NMR study of  $d8$ - $\text{Cu}[\text{N}(\text{CN})_2]\text{Br}$  is reported. Because of the low-temperature phase separation into the metallic (superconducting) and magnetic insulating phases, NMR spectra are well separated, which enabled us to examine separately the magnetic characters of the respective phases just on both sides of the Mott transition. In the metallic side, the enhanced pseudogapped behavior is uncovered, and in the insulating side the spin structure is determined for the first time.

The single crystals were grown by the standard chemical oxidation method with the use of the BEDT-TTF molecules where the hydrogenous in the ethylene groups are fully deuterated and the central double-bonded carbons are enriched by  $^{13}\text{C}$  isotopes [see Fig. 1(a)]. A crystal used in the present study is  $2\text{ mm} \times 2\text{ mm} \times 3\text{ mm}$  in size and 10 mg in weight. The crystal axes were identified by the x-ray diffraction measurements. In the  $^{13}\text{C}$  NMR measurements, an external field of 80.3 kOe was applied parallel to the  $a$  axis. Note that the conducting layer is the  $ac$  plane; that is, the applied field is parallel to the layer [see Fig. 1(b)]. As found for  $h8$ - $\text{Cu}[\text{N}(\text{CN})_2]\text{Br}$  by De Soto *et al.* [5], the  $^{13}\text{C}$  spectral splitting due to the nuclear dipole coupling vanishes in this field configuration,

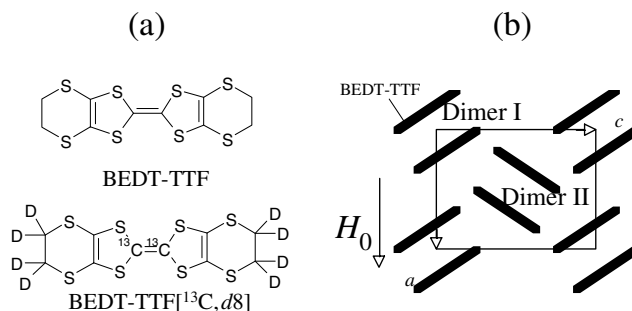


FIG. 1. (a) BEDT-TTF molecules with and without isotope substitutions. (b)  $\kappa$ -type BEDT-TTF molecular arrangement within the conducting  $ac$  plane.

because this particular angle between the external field and the  $^{13}\text{C} = ^{13}\text{C}$  direction forms the “magic angle.” Moreover, all of the BEDT-TTF molecules become equivalent against the field parallel to the  $a$  axis. So, one expects to observe only two NMR lines which come from the two neighboring  $^{13}\text{C}$  sites with different hyperfine tensors in a BEDT-TTF molecule. Figures 2(a) and 2(b) show the  $^{13}\text{C}$  NMR spectra. As expected, the observed spectra comprise two peaks at high temperatures. Hereafter, the lines with the smaller and larger shifts are called *A* and *B*, respectively. The relaxation rate was determined for Line A. As for the AFI phase emerging at low temperatures (see below), it was determined at the peak position of the spectra.

With temperature decreased, the spectra show steplike broadening around 150 K and further gradual broadening starts below 70 K similarly to the case of  $h8\text{-Cu}[\text{N}(\text{CN})_2]\text{-Br}$  [3,5], as is seen in the temperature dependence of the linewidth for *A* and *B* lines plotted in Fig. 2(c). While for  $h8\text{-Cu}[\text{N}(\text{CN})_2]\text{Br}$  the line-broadening levels off around 50 K, where the nonmetal-to-metal crossover occurs [5], the broadening for the present  $d8\text{-Cu}[\text{N}(\text{CN})_2]\text{Br}$  continues down 32 K with the two-peak structure kept. It is considered as the manifestation of the growing antiferromagnetic short-range order. Then, the line shape becomes rather complicated around 30 K and then splits to two components in quite different frequency regions at low temperatures. One stays in the shift range of Fig. 2(a). Its shift

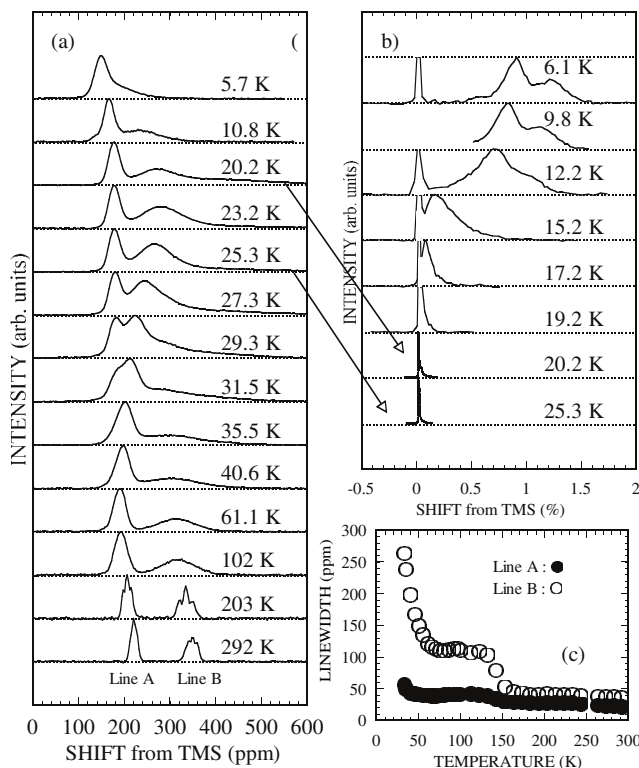


FIG. 2.  $^{13}\text{C}$  NMR spectra of a single crystal  $d8\text{-Cu}[\text{N}(\text{CN})_2]\text{Br}$  in shift ranges of hundreds of ppm (a) and of percent (b). (c) Temperature dependence of linewidth above 30 K.

and  $1/T_1$  steeply decrease around 11 K due to the superconducting transition as described below. The other begins to be out of the range of Fig. 2(a) below  $\sim 20$  K and gets to have a huge shift of percent order at lower temperatures as seen in Fig. 2(b) [12]. This shows the generation of local field, which indicates the magnetic ordering. Indeed, the divergence of  $1/T_1T$  is observed at 15 K as described below. From these behaviors, we conclude that the two spectral components separated below 30 K are from the metallic phase, which undergoes the superconducting transition at 11 K, and from the insulating phase, which shows the antiferromagnetic transition at 15 K. It is noted that the recovery of the nuclear magnetization was a single-exponential function over one decade above 30 K and was also the case for each phase below 30 K. These facts indicate that the system enters into a two-phase regime which is a consequence of the first-order character of the Mott transition driven by physical or chemical pressure. It is seen that Line-A separation occurs with comparable intensities at 29.3 and 27.3 K, meaning that the separated phases have comparable volume fractions at these temperatures. The two-phase spectra become so well separated below 15 K that the relative intensity of the AF phase is found to increase from 60% at 15.2 K to 85% at 5.7 K. According to the  $T$ - $P$  phase diagram obtained from the pressure study of the  $\text{Cu}[\text{N}(\text{CN})_2]\text{Cl}$  salt by Lefebvre *et al.* [10], the first-order Mott transition line running along the  $T$  axis is inclined and has an upper endpoint around 30 K. The present results that the NMR signal separation starts around 30 K and the volume fraction of the AFI phase increases with temperature lowered are considered to reflect the two distinctive features of the phase diagram.

The spin structure in the AF phase is deduced from two distinct features in the spectra at the lowest temperatures of 6.1 K [see Fig. 2(b)]. The first is the doubly peaked structure. The second is the spectral shift only to the positive frequency side by  $\sim 1\%$  corresponding to  $\sim 0.9$  MHz. We confirmed that there is no signal in the negative frequency side down to  $-2\%$  corresponding to  $-2$  MHz. These spectral features are in strong contrast to the case of the nesting-driven incommensurate SDW where the spectra have a wide and continuous distribution of resonance frequency symmetrically extended around the origin of shift. In the typical case of the sinusoidal spin-density modulation, the spectrum forms a U-shape, as was observed in  $(\text{TMTSF})_2\text{PF}_6$  [13]. So, the present result shows that the magnetic structure of this system is commensurate.

Considering the symmetry of the crystal structure and the susceptibility behavior in addition to the spectral characteristics (the double peak and the one-sided shift), the possible spin configurations are restricted as follows. Since the inversion symmetry exists on the center of the BEDT-TTF dimer, the two equivalent molecules in a dimer have the same hyperfine tensors. If the spin configuration within a dimer was antiparallel, the spectra would be split to positive and negative frequency sides according to the opposite

hyperfine fields. The observation of the one-sided spectral shift excludes this antiparallel configuration within the dimer. Furthermore, the maintenance of the double-peaked structure even in the magnetic phase means that the magnitude of the moment is the same on all the molecules. Namely, the spin is parallel and equally populated on both molecules in a dimer. Thus, the dimer spin can be regarded as a spin unit. The spectral shift is proportional to the hyperfine field component parallel to the applied field. At first sight, the one-sided spectral shift seems to indicate that the dimer spins are ferromagnetically ordered. However, it is not so straightforward, because there are differently oriented dimers (Dimers I and II in Fig. 1(b)), and the hyperfine tensors at the  $^{13}\text{C}$  site are anisotropic. What the experimental result indicates is that the  $a$ -axis component of the hyperfine field made by the ordered moment is the same for all the molecules. Its first consequence is that the dimer spin configuration is ferromagnetic within the Dimer-I sublattice or the Dimer-II one. Therefore, the issue is focused on the orientation relation between the spins on Dimer I and Dimer II. The  $\kappa$ -(BEDT-TTF) $_2\text{Cu}[\text{N}(\text{CN})_2]\text{Br}$  salt has  $Pnma$  symmetry [14]. The two dimers within a layer are connected by the  $ab$  plane mirror operation with the  $a$ -axis translation. Noting that by this mirror operation of the dimer spin the  $a$ -axis and  $b$ -axis components of the dimer spin and the hyperfine field are maintained but the  $c$ -axis component is reversed, the dimer spin configurations which give the same  $a$ -axis component of the hyperfine field are restricted to the following three types as shown in Fig. 3 with the spectral profiles calculated with the use of the hyperfine coupling tensors [15]: (i) ferromagnetic align-

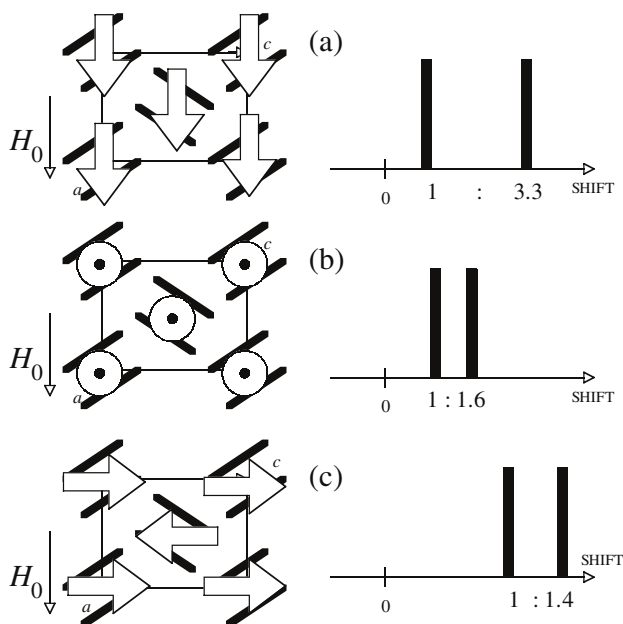


FIG. 3. The possible spin configurations (left) and calculated spectral profiles (right) for explanation of the one-sided shift of spectra below  $T_N$ .

ment directed to the  $a$  axis [Fig. 3(a)]; (ii) ferromagnetic alignment directed to the  $b$  axis with the out-of-plane antiferromagnetic configuration in consequence of the mirror symmetry with respect to the  $ac$  plane [Fig. 3(b)]; and (iii) antiferromagnetic alignment directed to the  $c$  axis [Fig. 3(c)]. The magnetic susceptibility of this system is insensitive to temperature down to about 100 K and decreases gradually with temperature down to 15 K where the magnetic transition occurs. This behavior indicates that the strongest exchange interaction is not ferromagnetic but antiferromagnetic [16]. We did not see the NMR rf amplification effect which is encountered in the ferromagnetically ordered phase. Thus, the cases of (i) and (ii) are ruled out. Indeed, if the case of (i) occurs, the spectral shift is determined by the diagonal ( $a, a$ ) component of the hyperfine coupling tensor, which is more than 3 times different between the two neighboring carbon sites [15]. This ratio contradicts the observed shift ratio of the two lines that is 1.5. After all, the dimer spin is concluded to have the simplest commensurate antiferromagnetic configuration of (iii), as depicted in Fig. 3(c). Under the present measurement of 80 kOe, the spin should be flopped [6]. The concluded spin configuration of Fig. 3(c) is consistently among the flopped configurations. This is consistent with a picture of the Mott insulator where a conduction hole is localized on a dimer.

The amplitude of the ordered moment is estimated from the spectral shift in Fig. 2(b) and the knowledge of the hyperfine tensor determined in [5]. If a moment of  $1.0\mu_B$  stands on a dimer and is directed to the  $c$  axis, the  $a$ -axis component of the hyperfine field for the site giving Line A is 2.8 kOe, which corresponds to a spectral shift of 3.0 MHz. So, the observed shift of 0.78 MHz yields a moment value of  $0.26\mu_B/\text{dimer}$  at 6.1 K. This value is smaller than that of  $\kappa$ -(BEDT-TTF) $_2\text{Cu}[\text{N}(\text{CN})_2]\text{Cl}$  (greater than  $0.4\mu_B$ ) [6], which is situated farther from the  $M-I$  boundary than  $d8\text{-Cu}[\text{N}(\text{CN})_2]\text{Br}$  salt. It is noted that the Néel temperature of the  $d8\text{-Cu}[\text{N}(\text{CN})_2]\text{Br}$  is also lower than that of the  $\text{Cu}[\text{N}(\text{CN})_2]\text{Cl}$  salt.

Figure 4(a) shows the temperature dependence of  $1/T_1T$ . The  $1/T_1T$  increases gradually with temperature decreased from 300 K. This behavior is just what was found for  $h8\text{-Cu}[\text{N}(\text{CN})_2]\text{Br}$  and  $\text{Cu}[\text{N}(\text{CN})_2]\text{Cl}$  salts. As discussed before, this common behavior is attributed to the growth of the antiferromagnetic spin fluctuations. The spectral separation below 30 K according to the SC and AFI phase separation allows us to measure the relaxation rate of each phase separately. The gradual increase in  $1/T_1T$  continuously grows into a steep increase in the AFI phase at lower temperatures, implying that this phase is a low-temperature continuation of the high-temperature single phase. A divergent peak of  $1/T_1T$  at 15 K where the spectrum also shifts drastically is an additional evidence of the AF transition. The whole feature of  $1/T_1T$  is the same as for the Mott insulator,  $X = \text{Cu}[\text{N}(\text{CN})_2]\text{Cl}$  salt, except for the Néel temperature.

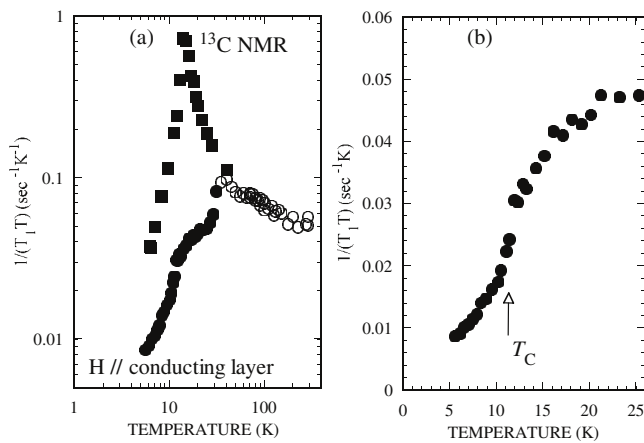


FIG. 4. (a) Temperature dependence of  $^{13}\text{C}$  NMR  $1/T_1T$  of the SC phase (closed circles) and the AFI phase (closed squares) below 30 K and of the high temperature phase (open circles) above 30 K. (b) Temperature dependence of  $1/T_1T$  of the SC phase at low temperatures in linear scales.

The other part of the spectra staying in a range of  $\sim 100\text{--}300$  ppm has the contrasting behavior. Around 30 K just after the signal separation,  $1/T_1T$  shows a sudden drop, which indicates depression of the AF spin fluctuations. The turnabout of the  $1/T_1T$  variation is also seen for  $h8\text{-Cu}[\text{N}(\text{CN})_2]\text{Br}$  around 45 K, which coincides with the inflection point of the metal-nonmetal resistivity crossover. The present result means that the crossover temperature is decreased to 30 K for  $d8\text{-Cu}[\text{N}(\text{CN})_2]\text{Br}$ , which is closely approaching the Mott boundary. The drop in  $1/T_1T$  at 30 K is so steep as to suggest the discontinuous transition although this possibility needs further experimental support. An additional intriguing feature is the anomalous decrease of  $1/T_1T$  below 30 K as shown in Fig. 4(b). Since the SC transition temperature of  $d8\text{-Cu}[\text{N}(\text{CN})_2]\text{Br}$  is 11 K according to the ac susceptibility measurements [11,17,18], it turns out that the decrease in  $1/T_1T$  begins at much higher temperatures than  $T_c$  and becomes steeper with temperature approaching  $T_c$ . Although  $1/T_1T$  decreases with temperature also for  $h8\text{-Cu}[\text{N}(\text{CN})_2]\text{Br}$ , the feature is much more prominent in the present phase. The decrease is too steep to observe a clear kink associated with the SC transition at  $T_c$ . This feature is similar to the so-called pseudogap behavior observed for the underdoped high- $T_c$  cuprates [19]. Although its origin is still controversial, the present observation can be addressed as the pseudogap which may have the common nature to the cuprates. It is interesting that the bandwidth controlled organics and the band-filling controlled cuprates share one of the most mysterious features in the vicinity of the Mott transition. The sharpened nonmetal-metal crossover and the enhanced pseudogap characterizes the metallic side of the Mott transition.

The observed two phases are the continuations from the SC phase of  $h8\text{-Cu}[\text{N}(\text{CN})_2]\text{Br}$  and the AFI phase of

$\text{Cu}[\text{N}(\text{CN})_2]\text{Cl}$ , respectively. The two continuations meet on the present system,  $d8\text{-Cu}[\text{N}(\text{CN})_2]\text{Br}$ . From the present results, we conclude that the pseudogapped SC phase with  $T_c$  of 11 K abuts on the commensurate AF phase with  $T_N$  of 15 K in the two-dimensional organic conductors. The fact that both phases have finite order parameters as measured by  $T_c$ ,  $T_N$ , and AF moment on the phase boundary means that the Mott transition is of the first order.

The authors thank H. Taniguchi for the x-ray measurement, and K. Kato and T. Takayama for the technical support. This work is supported by the PRESTO program from JST Corporation and by Grant-in-Aid for Scientific Research from the Ministry of Education, Science and Sports, Japan.

- [1] H. Kino and H. Fukuyama, J. Phys. Soc. Jpn. **64**, 2726 (1995).
- [2] K. Kanoda, Hyperfine Interact. **104**, 235 (1997); Physica (Amsterdam) **282C–287C**, 299 (1997).
- [3] H. Mayaffre *et al.*, Europhys. Lett. **28**, 205 (1994); Phys. Rev. Lett. **75**, 3586 (1995).
- [4] A. Kawamoto *et al.*, Phys. Rev. Lett. **74**, 3455 (1995); Phys. Rev. B **52**, 15 522 (1995).
- [5] S. M. De Soto *et al.*, Phys. Rev. B **52**, 10 364 (1995).
- [6] K. Miyagawa *et al.*, Phys. Rev. Lett. **75**, 1174 (1995).
- [7] J. Williams *et al.*, Inorg. Chem. **29**, 3272 (1990).
- [8] Yu. V. Sushko and K. Andres, Phys. Rev. B **47**, 330 (1993).
- [9] H. Ito *et al.*, J. Phys. Soc. Jpn. **65**, 2987 (1996).
- [10] S. Lefebvre *et al.*, Phys. Rev. Lett. **85**, 5420 (2000).
- [11] A. Kawamoto, K. Miyagawa, and K. Kanoda, Phys. Rev. B **55**, 14 140 (1997).
- [12] In this case, the spectra were obtained as the signal intensities against the measurement frequency which was varied under the constant external field of 80.3 kOe, because the fast Fourier transform of the echo at a fixed frequency could not cover the whole range of the spectra.
- [13] E. Barthel *et al.*, Europhys. Lett. **21**, 87 (1993).
- [14] U. Geiser *et al.*, Physica (Amsterdam) **174C**, 475 (1991).
- [15] The representation of the hyperfine coupling tensor with the  $a$ ,  $b$ , and  $c$  crystal axes is obtained by rotation of the shift tensor represented with the molecular axes given in Ref. [5]. For example, the  $(a, a)$  components at the two carbon sites are 0.94 and 3.1 kOe/ $\mu_B \cdot$  dimer.
- [16] A slight spontaneous magnetization observed in the ordered state is understood to result from a tiny canting in the antiferromagnetic spin configurations. The canting angle is estimated at the order of  $0.1^\circ$  from the ferromagnetic component (less than  $3 \times 10^{-3} \mu_B$ ), which makes no influence on the present determination of the spin structure and moment.
- [17] H. Taniguchi, A. Kawamoto, and K. Kanoda, Phys. Rev. B **59**, 8424 (1999).
- [18] M. Tokumoto *et al.*, Mater. Res. Soc. Symp. Proc. **488**, 903 (1998).
- [19] For example, T. Timusk and B. Statt, Rep. Prog. Phys. **62**, 61 (1999).